

RESEARCH

Open Access



An optimized Langendorff-free method for isolation and characterization of primary adult cardiomyocytes

Azadeh Nikouee^{1,2†}, John Q. Yap^{1,2†}, David J. Rademacher^{3,4}, Matthew Kim^{1,2} and Qun Sophia Zang^{1,2,3*}

Abstract

Isolation of adult mouse cardiomyocytes is an essential technique for advancing our understanding of cardiac physiology and pathology, and for developing therapeutic strategies to improve cardiac health. Traditionally, cardiomyocytes are isolated from adult mouse hearts using the Langendorff perfusion method in which the heart is excised, cannulated, and retrogradely perfused through the aorta. While this method is highly effective for isolating cardiomyocytes, it requires specialized equipment and technical expertise. To address the challenges of the Langendorff perfusion method, researchers have developed a Langendorff-free technique for isolating cardiomyocytes. This Langendorff-free technique involves anterograde perfusion through the coronary vasculature by clamping the aorta and intraventricular injection. This method simplifies the experimental setup by decreasing the need for specialized equipment and eliminating the need for cannulation of the heart. Here, we introduce an updated Langendorff-free method for isolating adult mice cardiomyocytes that builds on the Langendorff-free protocols developed previously. In this method, the aorta is clamped in situ, and the heart is perfused using a peristaltic pump, water bath, and an injection needle. This simplicity makes cardiomyocyte isolation more accessible for researchers who are new to cardiomyocyte isolation or are working with limited resources. In this report, we provide a step-by-step description of our optimized protocol. In addition, we present example studies of analyzing mitochondrial structural and functional characteristics in untreated isolated cardiomyocytes and cardiomyocytes treated with the acute inflammatory stimulus lipopolysaccharide (LPS).

Keywords Inflammation, Cardiomyocytes, Mitochondria, ROS, Sepsis, Heart function

[†]Azadeh Nikouee and John Q. Yap contributed equally to this project and are thus recognized as co-first authors.

*Correspondence:
Qun Sophia Zang
qzang@luc.edu

¹Department of Surgery, 2160 S. 1st Ave, Maywood, IL 60153, USA

²Burn & Shock Trauma Research Institute, 2160 S. 1st Ave, Maywood, IL 60153, USA

³Department of Microbiology and Immunology, 2160 S. 1st Ave, Maywood, IL 60153, USA

⁴Core Microscopy Facility, Loyola University Chicago Stritch School of Medicine, 2160 S. 1st Ave, Maywood, IL 60153, USA

Introduction

Isolation of cardiomyocytes from adult mice is a commonly used technique in cardiovascular research, facilitating the mechanistic investigation of cardiac physiology and heart diseases at the cellular level. The traditional method of isolating primary cardiomyocytes utilizes the technique of retrograde heart perfusion and is known as the Langendorff heart perfusion model. This method was developed by Dr. Oscar Langendorff and his colleagues at the University of Rostock in Germany towards the end of the 19th century [1]. The procedure involves excising the heart, inserting a cannula into the aorta, and perfusing



the heart retrogradely with an oxygenated digestion solution through a specialized apparatus. This foundational work laid the groundwork for significant advancement in studying cardiac physiology and pathology under various conditions. Over the years, modifications and refinements to the Langendorff technique have been made to improve the isolation of cardiomyocytes from perfused hearts across various species, especially rodents [2, 3]. A major advancement came with the introduction of enzymatic digestion methods combined with Langendorff perfusion in the 20th century, utilizing enzymes such as collagenase to dissociate cardiac tissue into individual cells while maintaining cell viability and functionality [4].

While the Langendorff method of isolation has been instrumental in advancing cardiac research, it poses technical challenges due to its intricate nature and necessitates the use of specialized equipment, including a perfusion chamber, pressure transducer, and basic temperature control. Additionally, the cost of a basic Langendorff setup typically ranges from \$10,000 to \$20,000. To simplify cardiomyocyte isolation and reduce associated costs, recent innovations have led to the development of a Langendorff-free method for isolating adult mouse cardiomyocytes, achieving yields comparable to the traditional method [5, 6]. This approach involves clamping the aorta, excising the heart, placing it in a petri dish with a warm enzymatic digestion solution, and anterograde perfusion by left ventricular injection. The primary benefits of this method include the elimination of aortic cannulation and the reduced need for specialized equipment.

Based on published protocols [3, 5, 7], we have optimized the cardiomyocyte isolation procedure from adult mice to increase ease of handling and reproducibility of the results. This report details our protocol modifications and potential downstream applications, as described in the [Method](#) section. In the results presented herein, we focused on characterizing mitochondrial structure and function in isolated adult cardiomyocytes, reflecting our group's research emphasis [8–10]. Given that the heart has a significantly higher energy demand compared to other organs, and cardiomyocytes rely on functional mitochondria for energy production, mitochondrial health is a critical indicator of cardiomyocyte vitality [11, 12]. Additionally, we challenged isolated cardiomyocytes with the bacterial endotoxin, lipopolysaccharide (LPS), as an experimental model for studying cardiomyocyte response to inflammatory stress. This approach is particularly relevant for understanding the pathophysiology of cardiovascular diseases characterized by inflammation such as sepsis-induced cardiomyopathy, myocarditis, endocarditis and pericarditis and may inform the development of novel therapeutic strategies. The results presented herein show that our optimized protocol yields viable cardiomyocytes with preserved morphology and

functionality. Moreover, these cardiomyocytes exhibit a discernible response to acute inflammation, thereby offering a valuable tool for investigating cardiac physiology and pathology.

Results

A simplified protocol of isolating primary cardiomyocytes from adult mice

By using our simplified cardiomyocyte isolation protocol described in the [Method](#) section, we consistently achieve yields comparable to those obtained through the traditional Langendorff methods (Fig. 1). The resulting cardiomyocytes exhibit the characteristic rod-like shape, with intact nuclei and plasma membranes and well-preserved T-tubules, as shown in Fig. 1 and Video 1.

Transmission electron microscopy analysis of mitochondrial structure, lipid droplets, and autophagic response in isolated cardiomyocytes

Transmission electron microscopy (TEM) is a powerful imaging modality for assessing organelle structures at high resolution. Previously, our group used TEM to show that mice intraperitoneally injected with LPS displayed increased disruption of mitochondria cristae structure in cardiac tissue slices [10]. In this report, we examined whether an acute inflammatory challenge by LPS alters mitochondria morphology in cardiomyocytes isolated from wild type adult male mice untreated or treated with LPS (5 mg/kg) for 18 h. Cardiomyocyte viability data is provided in (Table 1).

We have optimized the procedure of preparing cardiomyocyte samples for TEM imaging based on previously published studies [13–15]. Experimental details are provided in the [Method](#) section. The isolated cardiomyocytes contain mitochondria with intact cristae, having consistent and uniform morphology throughout the mitochondrial network (Fig. 2A), suggesting that the mitochondria maintain a healthy physiological status post-isolation. Despite no significant alterations in the total mitochondrial area (Fig. 2B), cells isolated from animals treated with LPS presented a significant reduction in the number of mitochondria (Fig. 2C) and cristae occupancy percentage (Fig. 2D). Additionally, a significant increase in the percentage of mitochondria exhibiting disorganized cristae in response to LPS was detected (Fig. 2E), consistent with our previously published results demonstrating sepsis-induced mitochondrial damage in the heart [10, 16]. Furthermore, we observed a significant increase in the area occupied by lipid droplets in response to the LPS challenge (Fig. 2F), suggesting that LPS challenge may cause an accumulation of lipids stored in lipid droplets due to decreased metabolism of fatty acids. However, this hypothesis will need further evaluation in future studies. We also detected an LPS-induced

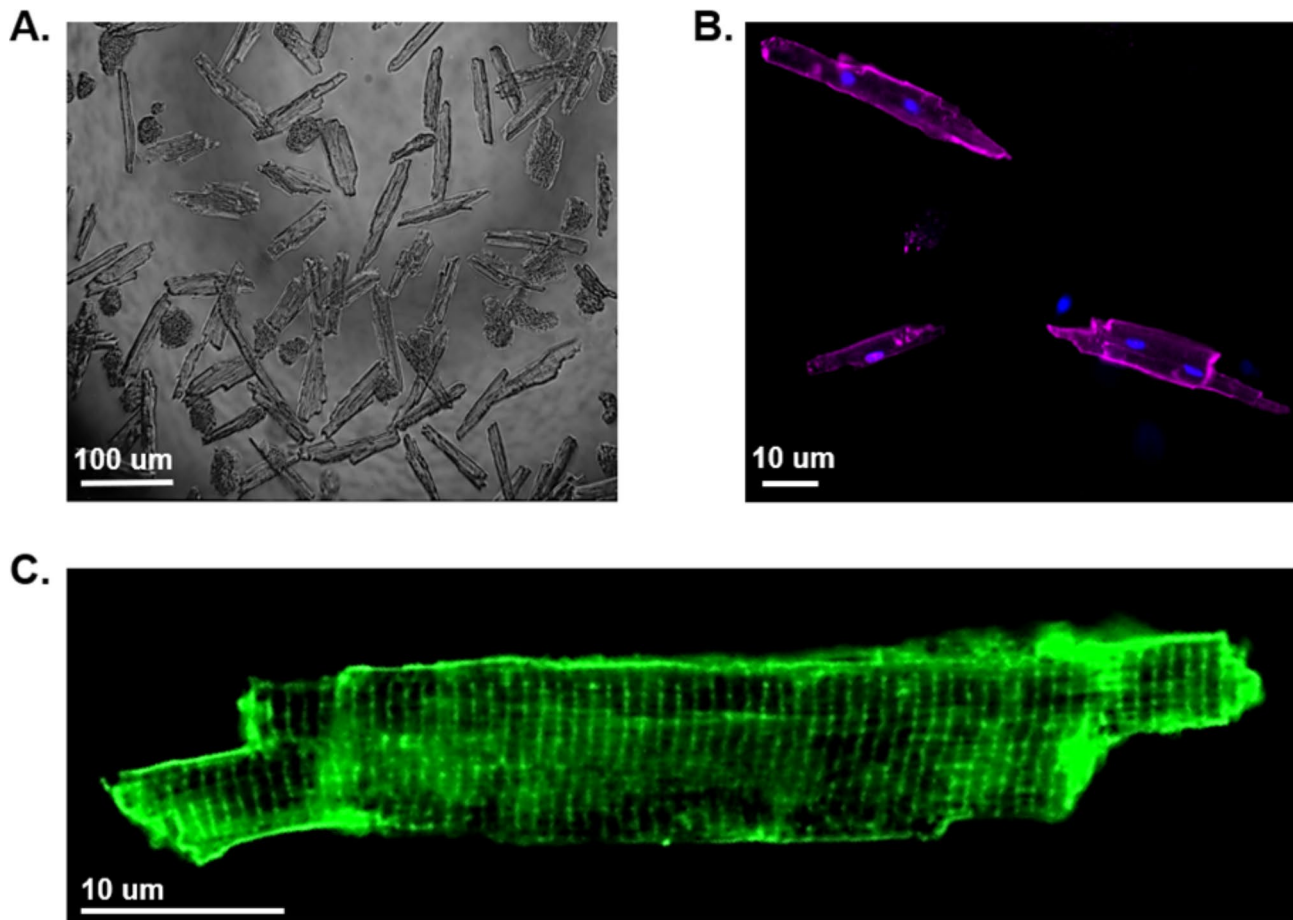


Fig. 1 Cardiomyocytes post-isolation. **A**) Brightfield image of isolated cardiomyocytes after plating. **B**) Confocal imaging of isolated cardiomyocytes stained with the cell membrane marker wheat germ agglutinin (WGA) (colored purple) and the nuclei marker DAPI (colored blue). **C**) Confocal imaging of isolated cardiomyocytes stained with the cell membrane and T-tubule marker Di-8-ANEPPS

Table 1

Condition	Biological Repl-icate 1	Biological Repl-icate 2	Biological Repl-icate 3	Mean Viabil-ity (%)	Standard Deviation
Untreated	90%	85%	80%	85%	4%
LPS	65%	68%	72%	68%	3%

increase in autophagy in the cardiomyocytes, signified by the formation of autophagosomes (Fig. 2G).

Measurement of mitochondrial membrane potential in isolated cardiomyocytes

To evaluate mitochondrial function in isolated cardiomyocytes, we chose to assess mitochondrial membrane potential, a crucial indicator for mitochondrial function and physiological fitness. To do this, isolated cardiomyocytes were incubated with JC-1 dye (Fig. 3A), which changes fluorescent properties based on the mitochondrial membrane potential. At low mitochondrial membrane potential, JC-1 takes on a monomeric form and emits a green fluorescence when excited. However, at

higher mitochondrial membrane potential, JC-1 molecules aggregate in the mitochondria and emit a red fluorescence when excited. A lower red-to-green ratio suggests that there is increased mitochondrial depolarization and mitochondrial dysfunction. In untreated isolated cardiomyocytes, we observed a high red-to-green ratio, indicating healthy cardiomyocytes with properly functioning mitochondria (Fig. 3B). However, LPS treatment significantly decreased the membrane potential by more than 50%, suggesting that mitochondrial function had been compromised in the cardiomyocytes (Fig. 3B).

Quantifying reactive oxygen species production in isolated cardiomyocytes

In healthy cardiomyocytes, low levels of reactive oxygen species (ROS) are generated when electrons that are leaked through the electron transport chain (ETC) interact with oxygen molecules to form superoxide radicals [17]. However, in unhealthy cardiomyocytes, mitochondrial dysfunction leads to increased leakage of electrons from the electron transport chain, resulting in increased

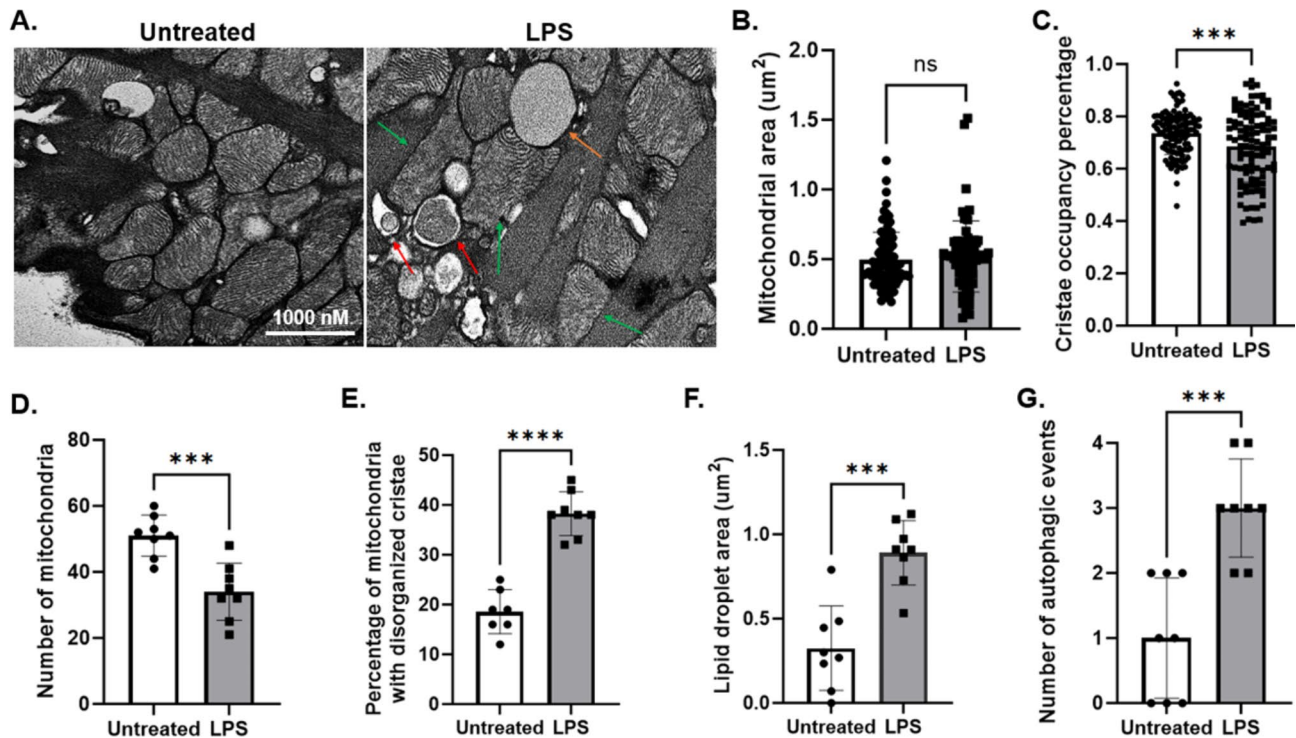


Fig. 2 Analysis of mitochondria morphology, lipid droplet accumulation and autophagy in isolated cardiomyocytes using TEM. **A**) TEM images of cardiomyocytes isolated from mice that were untreated or treated with LPS (5 mg/kg). Red arrows show autophagic events, the orange arrow shows a lipid droplet, and green arrows show mitochondria with disorganized cristae. Images are representative for $n = 3$ mice/group. **B**) Mitochondrial area per $50\mu\text{m}^2$. **C**) Percentage of cristae occupancy relative to total mitochondria area. **D**) Number of mitochondria per $50\mu\text{m}^2$. **E**) Percentage of mitochondria with disorganized cristae relative to the number of mitochondria per $50\mu\text{m}^2$. **F**) Lipid droplet area per $50\mu\text{m}^2$. **G**) Number of autophagic events per $50\mu\text{m}^2$. In **B-C**, values were expressed as mean \pm SD and analyzed by a Mann-Whitney U Test. In **D-G**, values were expressed as mean \pm SD and analyzed by a Student's *t*-test. Significance was determined by a *p*-value < 0.05 . A value of < 0.05 is indicated by a single asterisk (*), while values of < 0.005 , < 0.0005 , and < 0.00005 are denoted by two, three, and four asterisks (**, ***, ****), respectively

levels of ROS [18]. Treatment of cardiomyocytes with low concentrations of LPS increases ROS production [19]. To assess ROS production in isolated cardiomyocytes, we incubated cardiomyocytes in MitoSOX Red, a fluorescent dye specific for detecting superoxide production in mitochondria from live cells. Cardiomyocytes were counterstained with the mitochondrial marker, MitoTracker Green (Fig. 4A). Compared to the untreated cardiomyocytes, the fluorescent intensity of MitoSOX Red increased significantly in cardiomyocytes treated with LPS (Fig. 4B). This result is consistent with previous findings showing increased ROS production in cardiomyocytes during acute inflammation [20].

Discussion

Research in our laboratory has been focused on understanding the complex dynamics of sepsis-induced cardiomyopathy, with a particular interest in how acute inflammatory stimuli from infections impact the mitochondria and mitochondria-associated membranes within the myocardium [9, 10, 21]. Previously, we utilized TEM imaging to examine the ultrastructural details of the myocardium in cardiac tissue samples. Despite

the valuable insights gained, the entire process, from sample preparation to imaging and subsequent analysis, proved to be both time-consuming and resource-intensive. Moreover, the extensive nature of the sample preparation protocol increases the risk of introducing artifacts, thereby impacting the consistency and reliability of experimental outcomes. The procedure of tissue sample preparation starts with whole-heart perfusion, followed by dehydration and embedding steps, in which any tissue shrinkage or distortion could adversely affect the integrity of the ultrastructural information obtained from TEM images. Moreover, the presence of specialized structures, such as intercalated discs, along with the varied orientation of heart muscle fibers, further complicates the TEM imaging process and complicates the interpretation of imaging data.

This report details enhancements to the Langendorff-free method for isolating cardiomyocytes, resulting in improved ease of handling and highly reproducible isolation of viable cardiomyocytes from adult mouse models. In the original Langendorff-free method pioneered by Acker-Johnson et al. in 2016, the isolation process was simplified by anterogradely perfusing the heart after

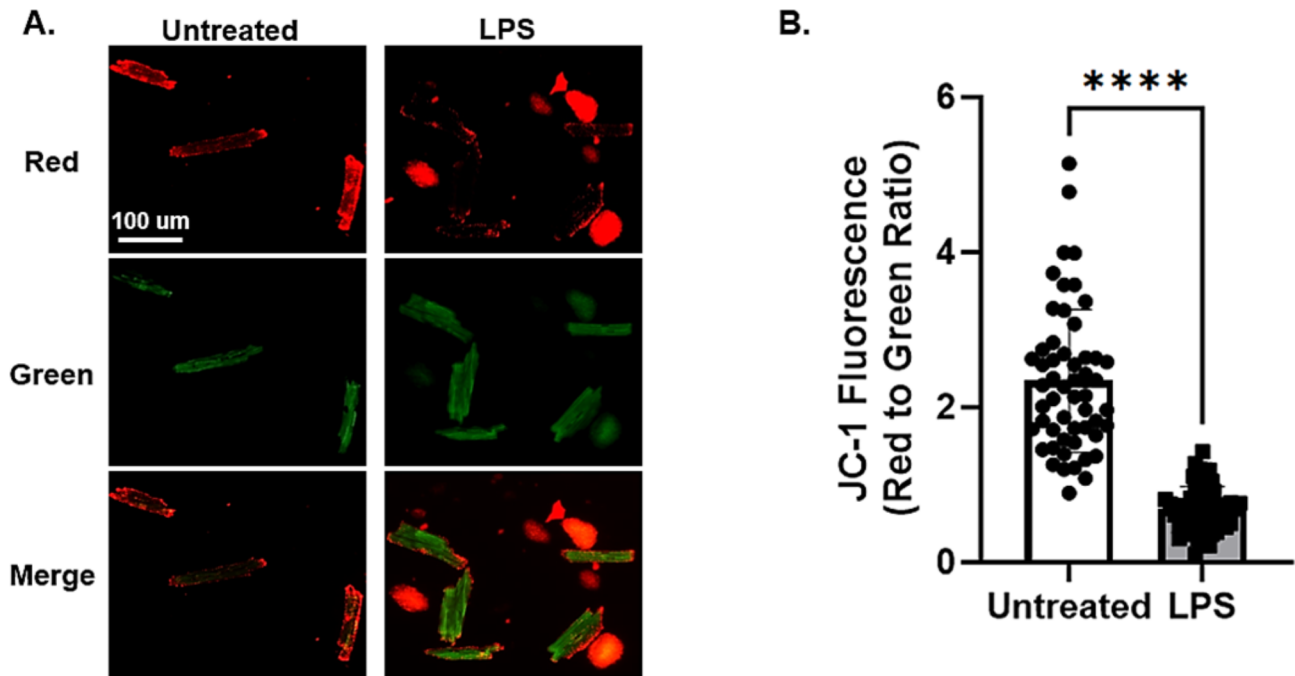


Fig. 3 Assessment of mitochondrial membrane potential in isolated cardiomyocytes. **(A)** Confocal imaging of JC-1 in untreated and LPS treated cardiomyocytes (10ng/ml). The scale bar in the upper left panel equals 100 μm and is valid for all panels. Images are representative of 50–70 cardiomyocytes analyzed from $n=3$ mice/group. **(B)** Quantification of JC-1 fluorescence in untreated and LPS treated cardiomyocytes. Values were expressed as mean \pm SD and analyzed by a Mann-Whitney U Test. Significance was determined by a p -value < 0.05 . **** indicates $p < 0.00005$

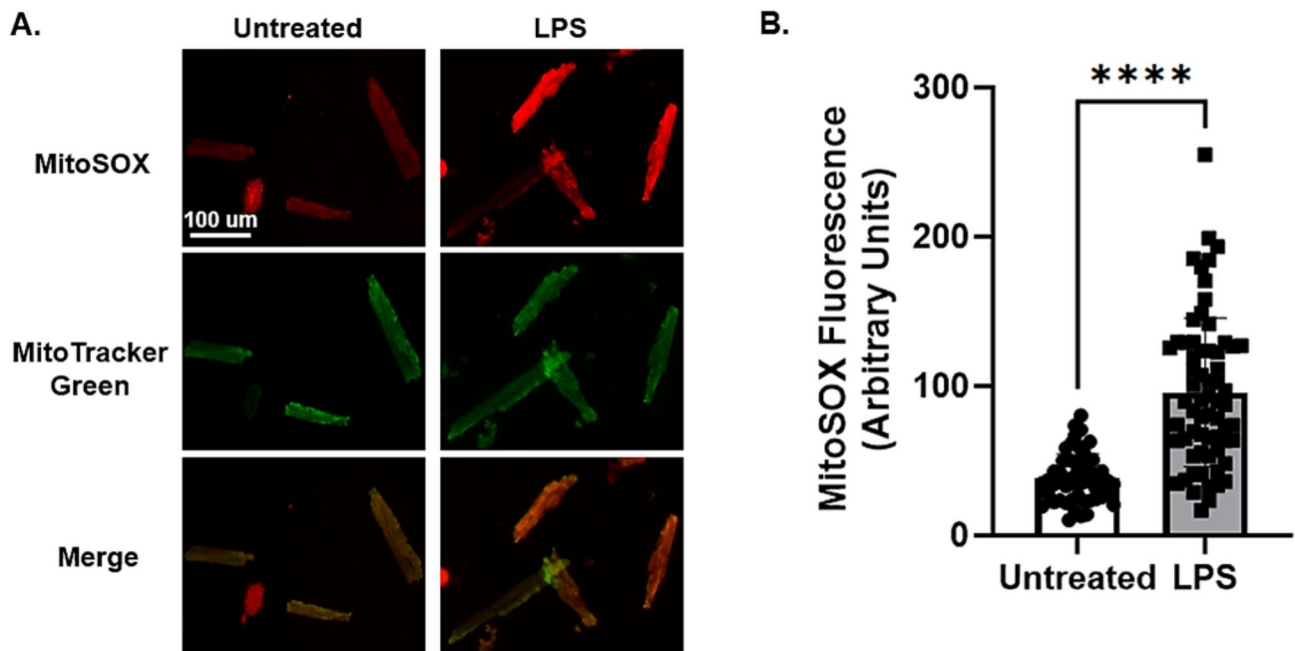


Fig. 4 Analysis of ROS production in isolated cardiomyocytes. **(A)** Confocal imaging of MitoSOX Red and MitoTracker Green in untreated and LPS treated (10 ng/ml) cardiomyocytes. The scale bar in the upper left panel equals 100 μm and is valid for all panels. Images are representative of 50–70 cardiomyocytes analyzed from $n=3$ mice/group. **(B)** Quantification of MitoSOX Red fluorescence in untreated and LPS treated cardiomyocytes. Images are representative of 50–70 cardiomyocytes analyzed from $n=3$ mice/group. Values were expressed as mean \pm SD and analyzed by a Mann-Whitney U Test. Significance was determined by a p -value < 0.05 . **** indicates $p < 0.00005$

clamping the aorta, eliminating the need for aortic cannulation [5]. However, a significant challenge of this Langendorff-free protocol is that manual injection of the digestive enzymes into the left ventricle requires an extremely steady hand for a prolonged period of time. In 2018, Omatsu-Kanbe et al. developed a modified version of the Acker-Johnson protocol that introduced a mechanical pump for consistent and precise delivery of the digestion buffer [22]. Additionally, Omatsu-Kanbe et al. standardized the depth of injection by marking the injection needle at 3 mm [22]. However, the Omatsu-Kanbe protocol involves clamping the aorta after the heart has been removed, a process that requires microscopic guidance and is more challenging than the *in situ* clamping used in the original Ackerman method. Our protocol combines the advantages of *in situ* clamping and mechanical perfusion, enhancing the ease of use and reproducibility of cardiomyocyte isolation.

Post-isolation, the cardiomyocytes demonstrated preservation of their physiological properties (Fig. 1). Subsequent TEM imaging of the isolated cell samples revealed findings that were in alignment with observations from intact heart tissue. As shown in Fig. 2, in addition to observing the ultrastructural morphology of mitochondria, we quantified the number of mitochondria, autophagy levels (autophagosomes and autolysosomes), and lipid droplets. Our analysis indicated that exposure to an acute inflammatory challenge, such as LPS, leads to severe mitochondrial damage characterized by disorganized cristae, reduced mitochondrial numbers, increased lipid droplets, and enhanced autophagic response. TEM analysis at the cellular level allows us to determine the intricate changes within the mitochondrial cristae, the surrounding membrane structures, and their interactions with lipid droplets in cardiomyocytes. We noticed that the lipid droplet features were significantly more evident in these cardiomyocyte images compared to whole heart tissue. This advantage is likely due to the fact that processing TEM samples prepared from isolated cells achieves a higher specificity in staining, thereby enhancing the contrast of ultrastructural components under TEM. Together, these results are consistent with previous findings seen in cardiomyocytes during acute inflammation, in which increased mitochondrial damage triggers activation of the autophagy/mitophagy processes [10], resulting in reduced mitochondrial numbers [10, 23]. The decrease in functional mitochondria has an effect on diminishing the capacity for lipid utilization, resulting in an accumulation of lipid droplets [24, 25].

Additionally, live cell-based detection using fluorescent labeling can be successfully applied in the isolated cardiomyocytes, which is another advantage compared to using heart tissue samples. In our study, we used JC-1 and MitoSOX to assess mitochondrial potential and

superoxide production, respectively. As shown in Figs. 3 and 4, we obtained results showing that LPS challenge caused a significant decrease in mitochondrial membrane potential and an increase in superoxide production, indicating the development of mitochondrial functional deficiency accompanied by oxidative stress. While these results demonstrate the effectiveness of this technique for downstream applications in studying cardiomyocyte and mitochondrial health and structure, the utility of this new method in preserving cardiomyocyte function—such as electrical and mechanical properties—following isolation will need to be evaluated in future studies.

In summary, we demonstrate an optimized method for isolating viable cardiomyocytes from adult mouse models. This simplified, straightforward method allows us to overcome the limitations associated with the traditional Langendorff method and sample preparation using cardiac tissue, reducing the time and resource demands, minimizing risk of artifacts, and enhancing our ability to obtain ultrastructural data with more defined details. The presented results we obtained from these isolated cardiomyocytes are consistent with findings obtained from the heart tissue. We anticipate that improving the methodology will help facilitate precise, reproducible, and insightful analysis of cardiomyocytes.

Method

Experimental animals

All methods are reported in accordance with ARRIVE guidelines 2.0 for the reporting of animal experiments [26]. Wild-type (WT) C57BL/6 mice were purchased from The Jackson Laboratory (Bar Harbor, ME) and housed at the in-campus mouse breeding core facility at Loyola University Chicago (LUC). Animals were conditioned in-house for 5–6 days after arrival with commercial diet and tap water available *ad libitum*. For the purposes of this study, male mice aged between 3 and 4 months were selected. All animal-related procedures described in this study underwent a comprehensive review and were conducted under the oversight of the LUC Institutional Animal Care and Use Committee. These procedures adhered to the standards outlined in the National Research Council's "Guide for the Care and Use of Laboratory Animals" when establishing animal research standards. For some experiments, LPS (MilliporeSigma, Burlington, MA; catalog number L3012) was injected intraperitoneally (i.p.), with each mouse individually weighed to determine the precise quantity of LPS required to achieve the specified doses as indicated in the figure legends. Experiments were conducted 18 h post LPS injection. Primary cardiomyocytes were isolated from the heart tissue according to the procedure described below. All methods are reported in accordance

Table 2

Compound	Final concentration (mmol/liter)	(mg) to be added	Catalog #
NaCl	130	7597.20	Sigma-Aldrich S9625
KCl	5	372.75	Sigma-Aldrich P4504
NaH ₂ PO ₄ ·H ₂ O	0.5	60.00	Sigma-Aldrich 71,496
HEPES	10	2383.00	Sigma-Aldrich H4034
Glucose	10	1251.50	Sigma-Aldrich G6152
BDM	10	1802.60	Sigma-Aldrich B0753
Taurine	10	1011.00	Sigma-Aldrich T0625

with ARRIVE guidelines (<https://arriveguidelines.org>) for the reporting of animal experiments.

Solutions made prior to the day of cardiomyocyte isolation 2× base buffer

To make the solution, add the components listed in Table 2 to 500 ml of distilled water. Gradually adjust the pH to 7.8 by adding NaOH dropwise. Once prepared, this solution can be stored at 4 °C for up to 2 weeks.

EDTA buffer

To prepare 250 ml 1× EDTA buffer solution, start by mixing 125 ml of a 2× base buffer with 125 ml of distilled water, and dissolve 365.3 mg of EDTA disodium dihydrate (Sigma Aldrich, E5134) into this 1× base buffer solution. Adjust the pH to 7.8 by adding NaOH dropwise, and filter the solution through a 0.2 µm filter to ensure sterility. This solution can be stored at 4 °C for up to 2 weeks. For each experiment, approximately 50 ml of this buffer will be required.

Perfusion buffer

To prepare 750 ml 1× perfusion buffer, start by mixing 375 ml of a 2× base buffer with 375 ml of distilled water, and dissolve 71.4 mg of MgCl₂ (Sigma Aldrich, M8266) into this 1× base buffer. Adjust the pH to 7.8 by adding NaOH dropwise, and filter the solution through a 0.2 µm filter to ensure its sterility. This prepared solution can be stored at 4 °C for up to 2 weeks.

Enzymes

Dilute 1000 mg of collagenase 2 (Worthington, LS004176), collagenase 4 (Worthington, LS004188), and protease XIV (Sigma Aldrich, P5147) separately in 20 ml of distilled water. Each enzyme should be prepared one at a time on ice and aliquoted into volumes of 525 µl for

Table 3

Enzyme	Final Concentration (mg/ml)	Volume required (ml)
Collagenase 2	0.5	0.5
Collagenase 4	0.5	0.5
Protease XIV	0.05	0.05
Perfusion Buffer		49

Table 4

Compound	Stock Concentration	Final Concentration	µl/1 ml media required
M199 (Thermo-Fisher Scientific, 11043023)			880
FBS	100%	10%	100
BDM	1 M	10 mM	10
P/S	100×	1×	10

*note: To make 1 M 2,3-Butanedione monoxime (BDM) solution, dissolve 0.101 g of BDM in 1 ml of distilled water and incubate the solution at 37 °C with gentle shaking until BDM is fully dissolved

collagenase 2 and collagenase 4 and 55 µl for protease XIV. Aliquots can be stored at -80 °C for up to 6 months.

Heparin

To prepare the heparin stock solution, dissolve 5 mg of heparin (Sigma Aldrich, H4784) in 1 ml of PBS. To prepare the working heparin solution, dilute 25 µl of the heparin stock solution in 75 µl of PBS. Both the stock and working heparin solutions can be stored at 4 °C.

Solutions made on the day of cardiomyocyte isolation

Digestion buffer

Digestion buffer can be prepared by mixing the ingredients listed in Table 3.

Stop buffer

Add 1 ml of fetal bovine serum (FBS) to 19 ml of perfusion buffer, and let the solution equilibrate to room temperature before use.

Plating media

Plating media can be prepared by mixing the components listed in Table 4. The total volume of plating media required will vary based on the quantity of downstream experiments planned. Prior to use, allow the solution to equilibrate to room temperature.

Calcium re-introduction solutions

Calcium re-introduction solutions can be prepared by mixing the components in Table 5. Prior to use, allow the solution to equilibrate to room temperature.

Table 5

Solution	ml for Buffer 1	ml for Buffer 2	ml for Buffer 3
Perfusion Buffer	6	4	2
Plating Media	2	4	6

Tyrode buffer

Dissolve 35.28 mg of CaCl₂·6H₂O (Sigma Aldrich, 21108) in 200 ml of perfusion buffer, and pass the solution through a 0.2 µm filter for sterilization. This solution can be stored at 4 °C for up to 2 weeks.

Preparation of cell culture plates

Coat 35 mm plates with 0.1 mg/mL poly-D-Lysine (PDL) (Sigma Aldrich, 6407) for 30 min at room temperature. Then, aspirate the PDL solution and allow the plates to dry for at least 30 min in a 37 °C incubator. Prior to cell plating, rinse the plates once with plating media.

Preparation of surgical equipment and area

Tubing preparation

One day prior to the experiment, flush the peristaltic pump tubing (Harvard Apparatus, 72–0668) with 70%

ethanol followed by water to ensure cleanliness. Allow the tubing to air dry completely.

Surgical area preparation

Clean the surgical area thoroughly with 70% ethanol before the procedure. Sterilize all surgical instruments as shown in Fig. 5A to maintain aseptic conditions.

Buffer preparation

- On the experiment day, prepare three sterile 50 ml conical tubes: one with 50 ml of EDTA solution and the other two with 50 ml of digestion buffer each. The second digestion buffer conical serves as a refill for the one connected to the pump.
- Place both the EDTA and digestion buffer solutions in a 37 °C water bath to reach the desired temperature. Once at 37 °C, introduce the peristaltic pump tubing into these solutions (Fig. 5B).

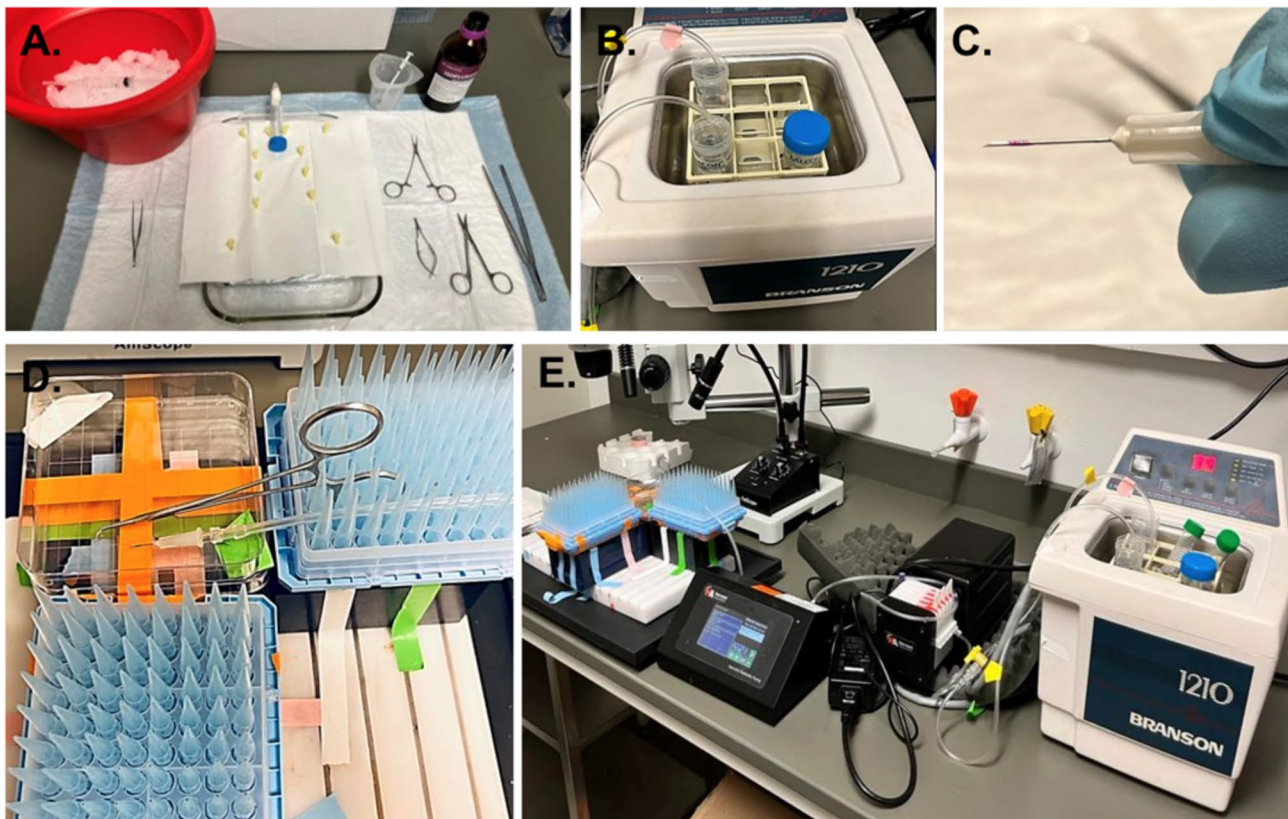


Fig. 5 Setup for cardiomyocyte isolation. **(A)** Surgical tools needed for heart excision, including a surgical table, a 5 ml syringe containing ice-cold EDTA buffer, tweezers, sharp-tipped scissors, Vannas scissors, and curved-ended Reynolds hemostatic forceps. **(B)** EDTA and digestion buffers in a 37 °C water bath for preparation. **(C)** Injection needles marked with nail polish to ensure penetration depth of only 3 mm into the heart. **(D)** A custom-made holder securely positions the injection needle and tubing. **(E)** An overview of the complete perfusion system

Pump and needle preparation

- Set the peristaltic pump (Harvard Apparatus, 70-7000) to 30 ml/min and allow approximately 10 ml of digestion buffer to circulate through the tubing to expel any air bubbles. Repeat the process with the EDTA buffer.
- To prevent the injection needles from being inserted too deeply, mark two 27G needles at a distance of 3 mm from the needle tip using colored nail polish (Fig. 5C).

Syringe and needle setup for ventricular injection

- Fill a sterile 5 ml syringe with 5 ml of cold EDTA buffer and attach one of the marked 27G needles. Keep the syringe on ice until use; this is intended for injection into the right ventricle to expel blood and halt cardiac contractions.
- Connect the other marked needle to the peristaltic pump tubing designated for heart injections and secure the setup in place (Fig. 5D). In this procedure, the tubing is steadily fixed into place using a holder made of P1000 tips taped in a refill wafer. The complete set up of the perfusion system is shown in Fig. 5E.

Cardiomyocyte isolation procedure

- Inject 50ul of working heparin solution intraperitoneally into the mouse and let the mouse rest for 10 min.
- Anesthetize the mouse by placing the animal in a glass container containing gauze moistened with isoflurane. Remove the mouse from the jar after one minute and confirm full anesthesia by verifying the

absence of a toe-pinch reflex. Maintain anesthesia by placing a nose cone containing gauze moistened with isoflurane over the mouth and nose of the mouse.

- After ensuring the mouse is fully anesthetized, open the chest cavity using sharp scissors. Clean the chest area with 70% ethanol and make an incision below the diaphragm. Locate the septum and gently elevate it to cut laterally below the ribs. Expose the diaphragm by cutting along the rib cage, then carefully slice the ribcage upwards and pin it back to reveal the heart (Fig. 6A, Video 2).
- To clear the heart of blood and cease its contraction, gently move the lungs aside, sever the inferior vena cava and the descending aorta with Vannas Spring Scissors (F.S.T, 91500-09), and inject 5 ml of ice-cold EDTA into the right ventricle using a syringe marked at 3 mm (Fig. 6B, Video 3).
- Clamp the aorta with Micro Hemostatic Forceps 12.5CM, 90 deg ang (WPI, 503360) to secure the heart before excision (Fig. 6C, Video 4).
- Remove the heart and place it in a 100 mm cell culture dish. Removal of the heart results in immediate euthanasia of the animal.
- Insert the 27G needle that is attached to the perfusion system into the heart (Fig. 7A, Video 5). Perfuse the heart with warm EDTA at 1.25 ml/min for 5 min, followed by digestion buffer at 1.5 ml/min for 60 min.
- Post-digestion, transfer the heart to a 35 mm dish with 1 ml of warm digestion buffer. Mince the tissue thoroughly with sharp tweezers (Fig. 7B).
- Move the minced tissue into a 50 ml tube containing 2 ml of warm digestion solution and incubate in a 37 °C water bath for 5 min. After 5 min, pipette the tissue/cell suspension up and down 20 times using a 3 ml transfer pipette. Place the tube in a 37 °C water

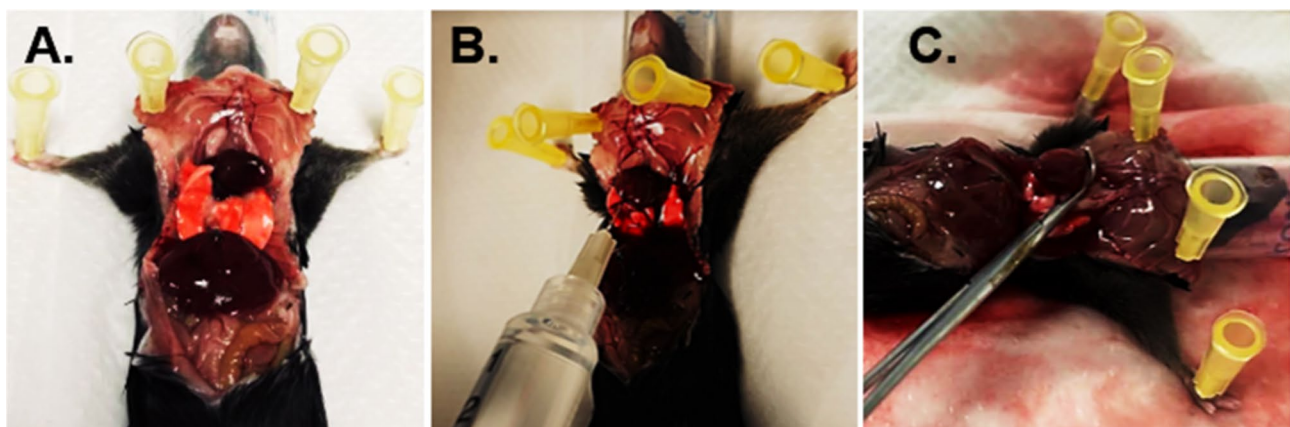


Fig. 6 Animal surgical procedure. (A) Chest cavity opened, exposing the heart; (B) Injection of EDTA buffer into the right ventricle; (C) Clamping the aorta

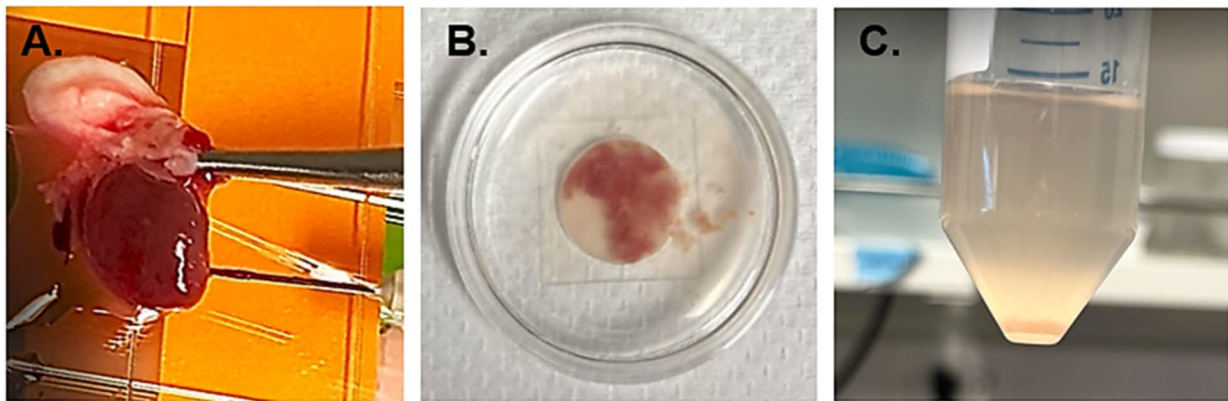


Fig. 7 Isolation of cardiomyocytes from the excised heart. **A**) Excised heart connected to the perfusion system via intraventricular injection. **B**) Heart tissue disassociation. **C**) Pellet of healthy cardiomyocytes

bath for 5 more minutes, then pipette the suspension up and down for another 20 times. At this point, the tissue should be fully digested. Add 5 ml of stop buffer and pipette the suspension up and down for another 5 times.

- j. Discard the supernatant, resuspend the cardiomyocyte pellet in calcium re-introduction wash buffer 1, and let settle for 15 min. Remove the supernatant and repeat the process with calcium re-introduction buffer 2 and buffer 3 sequentially. After the final settling, discard the supernatant, resuspend the cardiomyocyte pellet in 5–8 ml of plating media, and seed onto PDL-coated 35 mm glass-bottom dishes. Allow the cells to adhere at room temperature for 20 min.

Live cell imaging

Preparation of cells

- a. After the cells have adhered to the plates, the initial culture medium was replaced with fresh medium with or without LPS (10 ng/ml). Subsequently, the cardiomyocytes were incubated at 37 °C for 1 h.
- b. After the incubation, the cardiomyocytes were washed once with tyrode buffer and then incubated with the following dyes in tyrode buffer for 30 min at 37 °C: MitoTracker Green (100 nM, ThermoFisher Scientific, M7514) together with MitoSOX Red (5 μM, ThermoFisher Scientific, M36008), JC-1 (10 μg/ml ThermoFisher Scientific, T3168), or Di-8-ANEPPS (Invitrogen, D3167). For Di-8-ANEPPS, 5 mg of Di-8-ANEPPS was dissolved in 1 ml of DMSO. This stock solution can be stored at 4 °C. A working solution was prepared by mixing Di-8-ANEPPS stock and 20% Pluronic acid in a 1:1 ratio.

To prepare the dye solution, 0.5 μl of this working solution was added to 300 μl of Tyrode buffer.

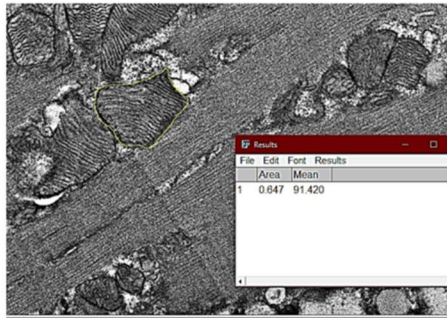
Imaging capture: Post-incubation, the cells were washed twice with tyrode buffer. Imaging was then performed using an LSM 510 confocal microscope, which features an Axio Observer Z1 motorized inverted microscope and Zen software (Carl Zeiss Microscopy), to capture images of the cells at 10x magnification. JC-1 fluorescence was excited at 560 nm to visualize the aggregated form (red fluorescence) and at 485 nm to detect the monomeric form (green fluorescence). Images of JC-1 red and green fluorescence were acquired with exposure times of 500 ms. MitoSOX fluorescence was excited at 510 nm and MitoTracker Green fluorescence was excited at 490 nm. Both MitoSOX and MitoTracker Green images were acquired with exposure times of 10,000 ms. Average fluorescence of the cell was analyzed using ImageJ. Only cardiomyocytes exhibiting rod shape morphology were analyzed.

Transmission electron microscopy (TEM) imaging

Sample fixation

- a. Cardiomyocytes were washed in phosphate-buffered saline (PBS) and then fixed in a solution of 2% paraformaldehyde (Electron Microscopy Sciences), 2.5% glutaraldehyde (Electron Microscopy Sciences), and 0.2% tannic acid (Ted Pella, Inc) in PBS for 1 h at room temperature.
- b. After extensive washing with deionized water, the samples were fixed in a solution of 1% osmium tetroxide and 1.5% potassium ferricyanide (Electron Microscopy Sciences) in deionized water for 1 h at room temperature in the dark.

- A.** Outline mitochondria using freehand tool → Analyze → Measure



- B.** Image → Adjust → Threshold → Select threshold → Apply → Set background to NaN → Outline mitochondria using freehand tool → Analyze → Measure

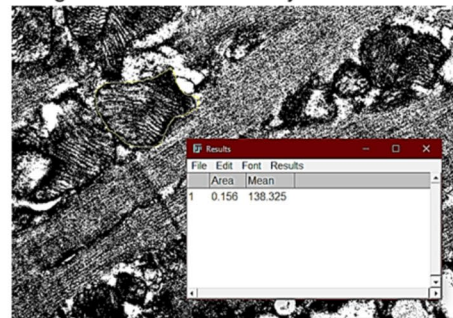


Fig. 8 Analysis of mitochondria area and cristae surface area from TEM images. **(A)** Calculating mitochondria area. **(B)** Calculating area unoccupied by mitochondrial cristae

Dehydration and post-fixation staining

The samples were immersed in 25% alcohol for 10 min followed by an incubation with 1% uranyl acetate in 50% alcohol for 1 h in the dark (i.e., *en bloc* uranyl acetate staining). Subsequently, the samples were incubated with 75% alcohol for 10 min, three changes of 95% alcohol for 10 min each, three changes of 100% alcohol for 10 min each, and 3 changes of propylene oxide (Electron Microscopy Sciences) for 10 min each.

Embedding

- The samples were embedded in a 1 to 1 ratio of propylene oxide to epoxy resin, comprised of a mixture of EMBED 812, nadic methyl anhydride, dodecyl succinic anhydride, and 2,4,6-Tris(dimethylaminomethyl)phenol, Electron Microscopy Sciences), for 12 h on a rotary mixer (Ted Pella, Inc.).
- The samples were then fully embedded in 100% epoxy resin for 12 h at room temperature on the rotary mixer, with a resin change followed by an additional 2-hour incubation. The epoxy resin was allowed to polymerize at 70 °C for 36 h and then allowed to cool to room temperature.

Sectioning

Ultrathin Sect. (90 nm) were prepared using an ultramicrotome (EM UC7, Leica Microsystems) then mounted on formvar- and carbon-coated 200 mesh copper grids (Electron Microscopy Sciences).

Section staining

Mounted samples were stained with filtered 1% uranyl acetate and Reynold's lead citrate prior to imaging.

Imaging capture

Imaging was performed using a Philips CM 120 transmission electron microscope (TSS Microscopy) equipped with a BioSprint 16 megapixel digital camera (Advanced Microscopy Techniques).

Semi-quantification analysis of TEM images

Images were properly scaled and quantitative analysis, including measurements of mitochondria number, area, cristae occupancy, disorganization of cristae, lipid droplet area, and autophagic events, was conducted using ImageJ software. Specifically, mitochondria with normal cristae were characterized by organized, densely packed membranes, whereas those with disorganized cristae were identified by swelling, fragmentation, or irregular shapes. Mitochondrial and lipid droplet areas were measured using the freehand tool (example shown in Fig. 8A). Cristae occupancy percentage was calculated by converting images to 32-bit, applying a threshold, and analyzing the outlined area unoccupied by cristae (Fig. 8B). The formula used was: Cristae occupancy percentage = (total mitochondrial area - area unoccupied by cristae) / total mitochondrial area × 100.

Statistics

The results are presented as the mean ± SEM, based on the specified number of experiments or mice. Statistical significance was assessed using a Mann-Whitney U Test or Student's t-test depending on data distribution. Differences were deemed statistically significant when $p \leq 0.05$.

Supplementary Information

The online version contains supplementary material available at <https://doi.org/10.1186/s12872-024-04256-5>.

- Supplementary Material 1
- Supplementary Material 2
- Supplementary Material 3

Supplementary Material 4

Supplementary Material 5

Author contributions

Conception: Q.S.Z.; methodology: A.N., J.Q.Y., D.J.R.; data curation: A.N., J.Q.Y., D.J.R.; experiments execution: A.N., J.Q.Y., D.J.R., M.K.; data analysis: J.Q.Y., Q.S.Z.; writing and revision: A.N., J.Q.Y., D.J.R., Q.S.Z. All authors have read and agreed to the published version of the manuscript.

Funding

This work is supported by NIH funding R21 AI178434, NIH R21 AI66913, and R01 GM111295 to Q.S.Z.

Data availability

Availability of data and materials: The results and images generated and/or analyzed during the current study are available from the corresponding author on reasonable request.

Declarations

Ethics approval and consent to participate

The animal study protocols were rigorously reviewed and received approval from the Institutional Animal Care and Use Committee (IACUC) at Loyola University Chicago. Our procedures strictly adhered to the guidelines outlined in the National Research Council's "Guide for the Care and Use of Laboratory Animals." All methods are reported in accordance with ARRIVE guidelines 2.0 for the reporting of animal experiments [26].

Consent for publication

All identifiable individuals have given their informed consent for the publication of data and images in this report.

Competing interests

The authors declare no competing interests.

Received: 19 March 2024 / Accepted: 14 October 2024

Published online: 15 November 2024

References

- Zimmer HG. The isolated perfused heart and its pioneers. *News Physiol Sci*. 1998;13:203–10. <https://doi.org/10.1152/physiologyonline.1998.13.4.203>. Epub 2001/06/08.
- Li H, Liu C, Bao M, Liu W, Nie Y, Lian H, Hu S. Optimized Langendorff perfusion system for cardiomyocyte isolation in adult mouse heart. *J Cell Mol Med*. 2020;24(24):14619–25. <https://doi.org/10.1111/jcmm.15773>. Epub 2020/11/05.
- Omatsu-Kanbe M, Fukunaga R, Mi X, Matsuura H. An Antegrade Perfusion Method for Cardiomyocyte Isolation from Mice. *J Vis Exp*. 2021(171). Epub 2021/06/08. <https://doi.org/10.3791/61866>. PubMed PMID: 34096909.
- Tian X, Gao M, Li A, Liu B, Jiang W, Qin Y, Gong G. Protocol for isolation of viable adult rat cardiomyocytes with high yield. *STAR Protoc*. 2020;1(2):100045. <https://doi.org/10.1016/j.xpro.2020.100045>. Epub 2020/10/29.
- Ackers-Johnson M, Li PY, Holmes AP, O'Brien SM, Pavlovic D, Foo RS. Simplified A. Langendorff-Free Method for concomitant isolation of viable Cardiac myocytes and nonmyocytes from the Adult Mouse Heart. *Circ Res*. 2016;119(8):909–20. <https://doi.org/10.1161/CIRCRESAHA.116.309202>. Epub 2016/08/10.
- Ackers-Johnson M, Foo RS. Langendorff-Free Isolation and Propagation of Adult Mouse Cardiomyocytes. *Methods Mol Biol*. 2019;1940:193–204. Epub 2019/02/23. https://doi.org/10.1007/978-1-4939-9086-3_14. PubMed PMID: 30788827.
- Farrugia GE, McLellan MA, Weeks KL, Matsumoto A, Cohen CD, Krstevski C, Gaynor TL, Parslow AC, McMullen JR, Pinto AR. A protocol for rapid and parallel isolation of myocytes and non-myocytes from multiple mouse hearts. *STAR Protoc*. 2021;2(4):100866. <https://doi.org/10.1016/j.xpro.2021.100866>. Epub 2021/10/15.
- Nikouee A, Kim M, Ding X, Sun Y, Zang QS. Beclin-1-Dependent Autophagy improves outcomes of Pneumonia-Induced Sepsis. *Front Cell Infect Microbiol*. 2021;11:706637. <https://doi.org/10.3389/fcimb.2021.706637>. Epub 2021/07/03.
- Sun Y, Cai Y, Qian S, Chiou H, Zang QS. Beclin-1 improves mitochondria-associated membranes in the heart during endotoxemia. *FASEB Bioadv*. 2021;3(3):123–35. <https://doi.org/10.1096/fba.2020-00039>. Epub 2021/03/19.
- Sun Y, Yao X, Zhang QJ, Zhu M, Liu ZP, Ci B, Xie Y, Carlson D, Rothermel BA, Sun Y, Levine B, Hill JA, Wolf SE, Minei JP, Zang QS. Beclin-1-Dependent Autophagy protects the Heart during Sepsis. *Circulation*. 2018;138(20):2247–62. <https://doi.org/10.1161/CIRCULATIONAHA.117.032821>. Epub 2018/06/02.
- Tian R, Colucci WS, Arany Z, Bachschmid MM, Ballinger SW, Boudina S, Bruce JE, Busija DW, Dikalov S, Dorn GW, Galis II, Gottlieb ZS, Kelly RA, Kitsis DP, Kohr RN, Levy MJ, Lewandowski D, McClung ED, Mochly-Rosen JM, O'Brien D, O'Rourke KD, Park B, Ping JY, Sack P, Sheu MN, Shi SS, Shiva Y, Wallace S, Weiss DC, Vernon RG, Wong HJ. Schwartz Longacre L. Unlocking the secrets of Mitochondria in the Cardiovascular System: path to a cure in Heart Failure-A report from the 2018 National Heart, Lung, and Blood Institute Workshop. *Circulation*. 2019;140(14):1205–16. <https://doi.org/10.1161/CIRCULATIONAHA.119.040551>. Epub 2019/11/27.
- Askin LPE, Tanriverdi O. Propionic Acidemia, Cardiomyopathies, and Arrhythmias. *J Clin Pract Res*. 2024;46(1):8. Epub 09.01.2024.
- Graham L, Orenstein JM. Processing tissue and cells for transmission electron microscopy in diagnostic pathology and research. *Nat Protoc*. 2007;2(10):2439–50. <https://doi.org/10.1038/nprot.2007.304>. Epub 2007/10/20.
- Gavini CK, Cook TM, Rademacher DJ, Mansuy-Aubert V. Hypothalamic C2-domain protein involved in MC4R trafficking and control of energy balance. *Metabolism*. 2020;102:153990. <https://doi.org/10.1016/j.metabol.2019.153990>. Epub 2019/11/02.
- Figge DA, Rahman I, Dougherty PJ, Rademacher DJ. Retrieval of contextual memories increases activity-regulated cytoskeleton-associated protein in the amygdala and hippocampus. *Brain Struct Funct*. 2013;218(5):1177–96. <https://doi.org/10.1007/s00429-012-0453-y>. Epub 2012/09/05.
- Zang QS, Martinez B, Yao X, Maass DL, Ma L, Wolf SE, Minei JP. Sepsis-induced cardiac mitochondrial dysfunction involves altered mitochondrial-localization of tyrosine kinase src and tyrosine phosphatase SHP2. *PLoS ONE*. 2012;7(8):e43424. <https://doi.org/10.1371/journal.pone.0043424>. Epub 2012/09/07.
- Moris D, Spartalis M, Tzatzaki E, Spartalis E, Karachaliou GS, Triantafyllis AS, Karaolanis GI, Tsilimigras DI, Theocharis S. The role of reactive oxygen species in myocardial redox signaling and regulation. *Ann Transl Med*. 2017;5(16):324. <https://doi.org/10.21037/atm.2017.06.17>. Epub 2017/09/02.
- Ray PD, Huang BW, Tsuji Y. Reactive oxygen species (ROS) homeostasis and redox regulation in cellular signaling. *Cell Signal*. 2012;24(5):981–90. <https://doi.org/10.1016/j.cellsig.2012.01.008>. Epub 2012/01/31.
- Joseph LC, Kokkinaki D, Valenti MC, Kim GJ, Barca E, Tomar D, Hoffman NE, Subramanyam P, Colecraft HM, Hirano M, Ratner AJ, Madesh M, Drosatos K, Morrow JP. Inhibition of NADPH oxidase 2 (NOX2) prevents sepsis-induced cardiomyopathy by improving calcium handling and mitochondrial function. *JCI Insight*. 2017;2(17). <https://doi.org/10.1172/jci.insight.94248>. Epub 2017/09/08.
- Mittal M, Siddiqui MR, Tran K, Reddy SP, Malik AB. Reactive oxygen species in inflammation and tissue injury. *Antioxid Redox Signal*. 2014;20(7):1126–67. <https://doi.org/10.1089/ars.2012.5149>. Epub 2013/09/03.
- Kim M, Nikouee A, Sun Y, Zhang QJ, Liu ZP, Zang QS. Evaluation of Parkin in the Regulation of Myocardial Mitochondria-Associated membranes and Cardiomyopathy during Endotoxemia. *Front Cell Dev Biol*. 2022;10:796061. <https://doi.org/10.3389/fcell.2022.796061>. Epub 2022/03/11.
- Omatsu-Kanbe M, Yoshioka K, Fukunaga R, Sagawa H, Matsuura H. A simple antegrade perfusion method for isolating viable single cardiomyocytes from neonatal to aged mice. *Physiol Rep*. 2018;6(9):e13688. <https://doi.org/10.14814/phy2.13688>. Epub 2018/04/27.
- Wang S, Long H, Hou L, Feng B, Ma Z, Wu Y, Zeng Y, Cai J, Zhang DW, Zhao G. The mitophagy pathway and its implications in human diseases. *Signal Transduct Target Ther*. 2023;8(1):304. <https://doi.org/10.1038/s41392-023-01503-7>. Epub 2023/08/16.
- Lee SJ, Zhang J, Choi AM, Kim HP. Mitochondrial dysfunction induces formation of lipid droplets as a generalized response to stress. *Oxid Med Cell Longev*. 2013. <https://doi.org/10.1155/2013/327167>. 2013:327167. Epub 2013/11/01.

25. Lemos GO, Torrinhas RS, Waitzberg DL, Nutrients. Physical Activity, and Mitochondrial Dysfunction in the Setting of Metabolic Syndrome. *Nutrients*. 2023;15(5). Epub 2023/03/12. <https://doi.org/10.3390/nu15051217>. PubMed PMID: 36904216; PMCID: PMC10004804.
26. Percie du Sert N, Ahluwalia A, Alam S, Avey MT, Baker M, Browne WJ, Clark A, Cuthill IC, Dirnagl U, Emerson M, Garner P, Holgate ST, Howells DW, Hurst V, Karp NA, Lasic SE, Lidster K, MacCallum CJ, Macleod M, Pearl EJ, Petersen OH, Rawle F, Reynolds P, Rooney K, Sena ES, Silberberg SD, Steckler T, Wurbel

H. Reporting animal research: explanation and elaboration for the ARRIVE guidelines 2.0. *PLoS Biol*. 2020;18(7):e3000411. <https://doi.org/10.1371/journal.pbio.3000411>. PubMed PMID: 32663221; PMCID: PMC7360025.

Publisher's note

Springer Nature remains neutral with regard to jurisdictional claims in published maps and institutional affiliations.